



CLICdp-Pub-2020-002  
18 February 2022

## Sensitivity to invisible Higgs boson decays at CLIC

K. Mekala, A. F. Zarnecki, B. Grzadkowski, M. Iglicki

*Faculty of Physics, University of Warsaw, Poland*

### Abstract

We studied the possibility of measuring invisible Higgs boson decays at CLIC running at 380 GeV and 1.5 TeV. The analysis is based on the WHIZARD event generation and fast simulation of the CLIC detector response with DELPHES. We considered  $e^+e^-$  background processes but also relevant  $\gamma\gamma$  and  $\gamma e^\pm$  interactions. The approach consisting of a two step analysis was used to optimize separation between signal and background processes. First, a set of preselection cuts was applied; then, multivariate analysis methods were employed to optimise the significance of observations. We estimated the expected limits on the invisible decays of the 125 GeV Higgs boson, as well as the cross section limits for production of an additional neutral Higgs-like scalar, assuming its invisible decays, as a function of its mass. Extracted model-independent branching ratio and cross section limits were then interpreted in the framework of the vector-fermion dark matter model to set limits on the mixing angle between the SM-like Higgs boson and the new scalar of the "dark sector".

*This work was carried out in the framework of the CLICdp Collaboration*

## 1 Introduction

All available experimental results seem to confirm that the new particle discovered in 2012 by the ATLAS and CMS experiments at LHC [1, 2] is the last missing constituent of the Standard Model (SM), the Higgs boson. The Standard Model predicts that the Higgs boson with a mass of about 125 GeV should decay predominantly to  $b\bar{b}$  (about 58% of all decays), but also to  $WW^*$  (21%),  $\tau\bar{\tau}$  (6,3%) or  $ZZ^*$  (2,6%)[3]. Some extensions of the Standard Model predict "invisible" Higgs boson decays – into new, not-observable particles. These particles could contribute to the Dark Matter (DM) density of the Universe. As of today, the best limits on invisible Higgs boson decays come from the CMS experiment – at 95% CL the branching fraction is less than 19%[4]. We study prospects for constraining invisible decays of the 125 GeV Higgs boson at a future experiment at CLIC.

Among many theories introducing DM particles and predicting invisible decays of the SM-like Higgs boson, there is a group of "Higgs-portal" models which assume existence of additional fundamental scalars. These new particles could mix with the SM-like Higgs and thus open new decay channels of the SM-like 125 GeV state into DM particles. The new scalars, if they are relatively light, could also be produced in  $e^+e^-$  collisions in the process corresponding to the Higgstrahlung process in the SM:  $e^+e^- \rightarrow ZH'$ . We extend our search for invisible decays of the SM-like Higgs boson to the search for production and invisible decays of a scalar particle,  $H'$ , with arbitrary mass. We then interpret our results in terms of the limits on the scalar sector mixing angle. We considered the *Vector-fermion dark matter* model (VFDM)[5, 6], a simple extension of the Standard Model with one extra scalar, two Majorana fermions and one gauge boson.

## 2 Event generation and fast simulation of the detector response

Results presented in this paper are based on a realistic simulation of events, including fast simulation of the CLICdet [7] detector response. Signal and background event samples were generated using WHIZARD 2.7.0 [8, 9], taking into account the beam energy profile expected for CLIC running at 380 GeV and 1.5 TeV. As the signal, we considered the Higgs-strahlung process: Higgs boson production (with decay into an invisible final state) together with a Z boson decaying into a quark-antiquark pair. For the background, we studied processes both with and without Higgs boson production. We also took into account the possible background contribution from  $\gamma\gamma$  and  $e^\pm\gamma$  interactions, where both beamstrahlung (BS) photons and photon radiation by the incoming electrons, as described by the Effective Photon Approximation (EPA)<sup>1</sup>, were taken into account. For CLIC running at 380 GeV, the same integrated luminosity of data is expected to be taken with negative and positive electron beam polarisation. We assume combined analysis of both samples, corresponding to  $1000 \text{ fb}^{-1}$  collected with unpolarised beam. At 1.5 TeV we consider the two electron beam polarisations separately, assuming  $2000 \text{ fb}^{-1}$  to be collected with -80% polarisation and  $500 \text{ fb}^{-1}$  with +80% polarisation<sup>2</sup> [10]. Cross sections for processes taken into account in the presented study<sup>3</sup> calculated by WHIZARD<sup>4</sup> and numbers of generated events are shown in Tables 1 (for 380 GeV running) and 2 (for 1.5 TeV).

To simulate detector response the fast simulation framework DELPHES was used [11]. Control cards prepared for the new detector model CLICdet [12] were modified to make Higgs particles 'invisible' in

<sup>1</sup>For generation of EPA events WHIZARD 2.8.3 was used, with a fix introduced to give correct matching of  $e^+e^-$  and  $\gamma^{EPA}e^\pm$  samples.

<sup>2</sup>For CLIC running at 1.5 TeV the integrated luminosity for  $\gamma^{BS}\gamma^{BS}$  interactions is assumed to be about 64% of the  $e^+e^-$  luminosity and for  $e^+\gamma^{BS}$  and  $\gamma^{BS}e^-$  interactions – about 75%.

<sup>3</sup>Not included are  $e^-e^+$  processes, in particular those with six fermions in the final state, eg.  $qqqq\ell\nu$  and  $qqqq\nu\nu$ , for which no events passed preselection cuts. For interactions involving EPA photons, only the process with the largest background contribution,  $\gamma e^\pm \rightarrow qq\nu$ , was considered, as  $\gamma\gamma$  and  $e^\pm\gamma$  interactions are dominated by BS photon interactions.

<sup>4</sup>Statistical uncertainty of cross-sections was below 1% and has been neglected.

Final state	$\sigma$ [fb]	$N_{GEN}$
qq	22145.90	2000000
ll	19917.10	1000000
qqqq	5075.88	500000
qqll	1718.07	200000
qqvv	317.44	300000
qqlv	5557.10	500000
qqlvvv	1.37	100000
$H_{SM} + qq$	82.23	100000
$H_{SM} + ll$	15.47	100000
$H_{SM} + vv$	54.54	100000
$\gamma^{BS} \gamma^{BS} \rightarrow qq$	1914.43	200000
$\gamma^{BS} \gamma^{BS} \rightarrow qqqq$	1.84	10000
$\gamma^{BS} \gamma^{BS} \rightarrow qqll$	33.04	10000
$\gamma^{BS} \gamma^{BS} \rightarrow qqlv$	0.72	10000
$\gamma^{BS} \gamma^{BS} \rightarrow qqvv$	0.03	10000
$\gamma^{BS} e^- \rightarrow qqv$	1418.31	300000
$\gamma^{BS} e^+ \rightarrow qqv$	1428.57	300000
$\gamma^{EPA} e^- \rightarrow qqv$	883.29	100000
$\gamma^{EPA} e^+ \rightarrow qqv$	883.41	100000
$H_{inv} + qq$		100000

Table 1: Cross sections,  $\sigma$ , and numbers of generated events,  $N_{GEN}$ , for each final state considered at 380 GeV; the reference cross section for  $H_{inv}qq$  channel is the SM Higgs boson production cross section for  $H_{SM}qq$  final state.

the simulation (ignored when generating detector response), so that the invisible Higgs boson decays can be modeled by defining the Higgs boson as stable in WHIZARD and PYTHIA. An event reconstruction begins with searching for isolated electrons, muons and photons (assuming reconstruction efficiency resulting from the full detector simulation). For CLICdet, DELPHES identifies isolated electrons and photons with energy of at least 2 GeV, and muons of 3 GeV. Jet clustering was carried out with the VLC[13] algorithm assuming minimal transverse jet momentum of 20 GeV. The values of  $R = 1.5$  for 380 GeV and  $R = 0.7$  for 1.5 TeV CLIC running were chosen as optimal for the VLC algorithm, with  $\beta = \gamma = 1$ . We require reconstruction of two hadronic jets, each with at least two charged particles. To take into account the effects of the beam-induced backgrounds, additional energy smearing is applied for jets reconstructed at 1.5 TeV: for central jets ( $|\eta| < 0.76$ ) the overlay events are expected to result in an additional 1% jet energy smearing, while for more forward jets ( $|\eta| \geq 0.76$ ) 5% smearing is assumed [12].<sup>5</sup>

<sup>5</sup>Jet energy smearing expected for CLIC running at 1.5 TeV (stage 2) and 3 TeV (stage 3) is implemented in DELPHES cards for CLICdet [12]. However, only the jet energy is smeared and the jet mass is assumed to be negligible. As the jet masses should not be neglected in the presented analysis, we use our own implementation of the jet energy smearing, with energy and mass of the jet scaled by the same factor.

Final state	$\sigma^{neg}$ [fb]	$\sigma^{pos}$ [fb]	$N_{GEN}$
qq	2873.36	1807.09	1000000
ll	1396.18	1218.17	1000000
qqqq	1970.67	265.47	1000000
qqll	2739.19	2570.04	1000000
qqvv	1520.11	187.32	1000000
qqlv	7054.84	1712.63	1000000
qqlvvv	40.15	5.39	100000
$H_{SM} + qq$	9.42	6.59	100000
$H_{SM} + ll$	31.65	22.09	100000
$H_{SM} + vv$	467.62	53.49	100000
$\gamma^{BS}\gamma^{BS} \rightarrow qq$	6030.48	6030.48	1000000
$\gamma^{BS}\gamma^{BS} \rightarrow qqqq$	6330.76	6330.76	100000
$\gamma^{BS}\gamma^{BS} \rightarrow qqll$	2791.48	2791.48	100000
$\gamma^{BS}\gamma^{BS} \rightarrow qqlv$	6697.38	6697.38	100000
$\gamma^{BS}\gamma^{BS} \rightarrow qqvv$	6.57	6.57	100000
$\gamma^{BS}e^- \rightarrow qqv$	28274.29	3141.6	1000000(neg.)/100000(pos.)
$\gamma^{BS}e^+ \rightarrow qqv$	15621.69	15621.69	1000000
$\gamma^{EPA}e^- \rightarrow qqv$	6616.77	735.20	300000
$\gamma^{EPA}e^+ \rightarrow qqv$	3677.43	3677.43	300000
$H_{inv} + qq$			100000

Table 2: Cross sections,  $\sigma^{neg}$  and  $\sigma^{pos}$ , for -80% and +80% electron beam polarisation, respectively, at 1.5 TeV CLIC, and numbers of generated events,  $N_{GEN}$ , for each considered final state; the reference cross sections for  $H_{inv}qq$  channel are the SM Higgs boson production cross sections for  $H_{SM}qq$  final state.

### 3 Signal event selection

#### 3.1 Preselection of events

A main purpose of the preselection is to remove all background events which are not consistent with the expected signature of the signal process. For the process  $e^+e^- \rightarrow HZ \rightarrow inv + qq$ , we expect to observe only two jets in the final state, with an invariant mass consistent with the mass of the Z boson. In the initial preselection step, all events which were not consistent with this signature were rejected. In particular, events with isolated leptons (electrons or muons) or isolated energetic photons (with energy greater than 5 GeV) were excluded. For a significant fraction of events, the difference between the energy sum of the reconstructed jets and the energy sum of all identified particles in the event was sizable, indicating an incomplete event reconstruction. To avoid such events, we require that this difference is less than 10 GeV.

In the next steps, quantities describing event topology were considered. First, we analyzed the distributions of parameters  $y_{23}$  and  $y_{34}$  describing the results of jet clustering with VLC algorithm. While the algorithm was forced to reconstruct two jets in each event, these distributions allowed us to distinguish actual two-jet events from events with a larger number of underlying jets in the final state. The distributions of  $-\log_{10}y_{23}$  and  $-\log_{10}y_{34}$  are shown in Figures 1(a) and 1(b), respectively. The double-peak structure clearly visible in the background sample of SM Higgs boson decays  $H_{SM}$  corresponds to pure two- and four-jet events. The distribution for the other background channels is more uniform. For the signal sample, with two hadronic jets, we expect values of  $y_{23}$  and  $y_{34}$  to be relatively small. We selected

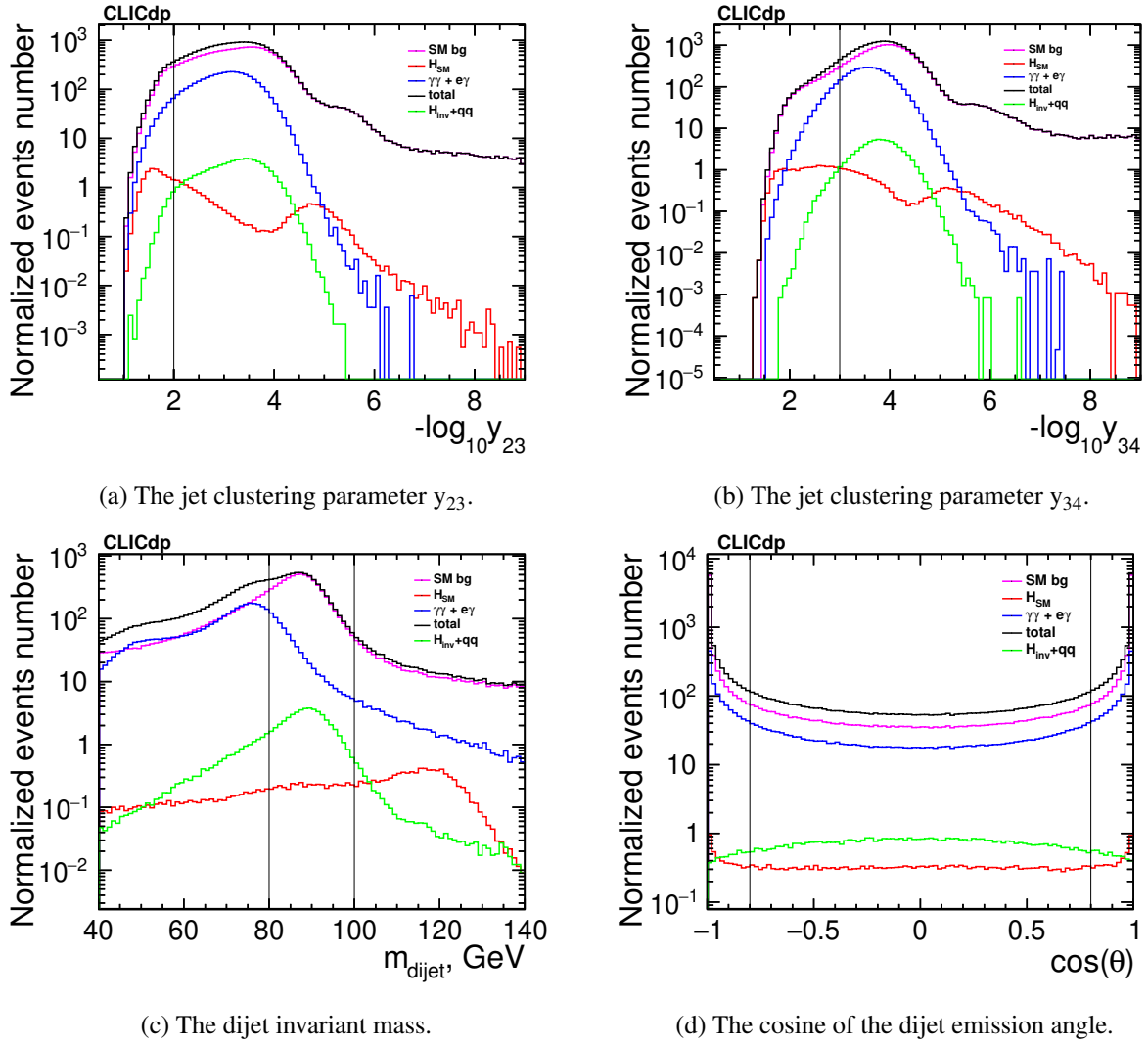


Figure 1: Distribution of preselection variables for different event samples considered: total background (black), SM background without Higgs particle production (pink), background of SM Higgs boson production and decays (red), photon interactions (blue) and signal (green); black vertical lines indicates preselection cuts, see text for details.

events for which  $y_{23} < 0.01$  ( $-\log_{10} y_{23} > 2.0$ ) and  $y_{34} < 0.001$  ( $-\log_{10} y_{34} > 3.0$ ).

The next quantity considered for the preselection of signal events was the invariant mass of the two jet final state –  $m_{\text{dijet}}$ . It should correspond to the mass of the Z boson, so only events for which this value was in the range of 80-100 GeV were selected for further analysis. The distribution of invariant masses for each channel is shown in the Figure 1(c). The peak visible in the channel of SM Higgs boson decays ( $H_{SM}$ ) around 120 GeV corresponds to the process  $e^+e^- \rightarrow HZ \rightarrow qq\nu\nu$  which, considering only its topology (two jets and missing energy), is indistinguishable from the signal. We also studied the distribution of the dijet emission angle,  $\theta$ , defined as the angle between the beam axis and a sum of the jet four-momenta (the emission angle of the Z boson for the signal events). For the majority of background events small emission angles are reconstructed, while for signal events the distribution is almost flat (angles close to  $90^\circ$  are slightly preferred). Therefore, events for which  $|\cos(\theta)|$  was greater than 0.8 were excluded from the analysis. The distribution of cosine of the angle  $\theta$  is shown in the Figure 1(d).

Final state	Efficiency	$N_{pre}$
without Higgs boson		
qq	0.08%	16831
ll	<0.01%	20
qqqq	<0.01%	51
qqll	0.02%	412
qqvv	20.47%	64974
qqlv	0.60%	33598
qqlvvv	1.32%	18
<b>Total:</b>	0.21%	115904
with Higgs boson decays described in the Standard Model		
$H_{SM} + qq$	<0.01%	41
$H_{SM} + ll$	0.01%	1
$H_{SM} + vv$	2.33%	1273
<b>Total:</b>	0.86%	1315
photon interactions		
$\gamma^{BS} \gamma^{BS} \rightarrow qq$	0.78%	9496
$\gamma^{BS} \gamma^{BS} \rightarrow qqll$	0.03%	6
$\gamma^{BS} \gamma^{BS} \rightarrow qqlv$	1.59%	7
$\gamma^{BS} \gamma^{BS} \rightarrow qqvv$	0.06%	1
$\gamma^{BS} \gamma^{BS} \rightarrow qqqq$	0.03%	1
$\gamma^{BS} e^- \rightarrow qqv$	6.73%	71596
$\gamma^{BS} e^+ \rightarrow qqv$	6.68%	71561
$\gamma^{EPA} e^- \rightarrow qqv$	6.32%	55833
$\gamma^{EPA} e^+ \rightarrow qqv$	6.20%	54771
<b>Total:</b>	5.11%	263270
signal		
$H_{inv} + qq$	43.56%	35779

Table 3: Efficiency and expected events number after preselection  $N_{pre}$  assuming integrated  $e^+e^-$  luminosity of  $1000 \text{ fb}^{-1}$  collected at 380 GeV for each considered final state. Results for the signal were calculated assuming SM Higgs boson production cross section and  $\text{BR}(H \rightarrow inv) = 100\%$ .

The results of the preselection are presented in Tables 3 and 4. Shown in Fig. 2 is the expected distribution of the so called recoil mass, the invariant mass of the Higgs boson produced together with the Z boson, after preselection cuts, reconstructed from the energy-momentum conservation for CLIC running at 380 GeV. For the background sample the distribution has two maxima: at around 300 GeV, which is the maximum recoil mass allowed (as we require two jets to have an invariant mass of at least 80 GeV) and at around 90 GeV, which is mainly due to invisible Z boson decays. For signal events, normalised in Fig. 2 to  $\text{BR}(H \rightarrow inv) = 10\%$ , the expected recoil mass distribution is consistent with the SM Higgs boson mass of 125 GeV. The slight shift of the maxima in the reconstructed recoil mass distributions towards higher mass values is most likely due to the influence of the beam energy spectra (a significant fraction of events takes place at energy scales lower than the nominal one).

Final state	Efficiency - p. neg.	$N_{pre}^{neg}$	Efficiency - p. pos.	$N_{pre}^{pos}$
without Higgs boson				
qq	0.07%	4040	0.08%	685
ll	<0.01%	6	<0.01%	2
qqqq	<0.01%	118	<0.01%	7
qqll	0.04%	2180	0.04%	458
qqvv	13.55%	412029	12.73%	11920
qqlv	1.47%	207723	2.29%	19622
qqlvvv	1.25%	1001	2.10%	57
<b>Total:</b>	1.76%	627097	0.84%	32751
with Higgs boson decays described in the Standard Model				
$H_{SM} + qq$	0.02%	3	<0.01%	0
$H_{SM} + ll$	0.11%	69	0.11%	12
$H_{SM} + vv$	2.34%	21903	2.50%	667
<b>Total:</b>	2.16%	21976	1.65%	680
photon interactions				
$\gamma^{BS} \gamma^{BS} \rightarrow qq$	0.21%	16541	0.22%	4221
$\gamma^{BS} \gamma^{BS} \rightarrow qqll$	0.04%	1501	0.04%	375
$\gamma^{BS} \gamma^{BS} \rightarrow qqlv$	0.32%	27518	0.32%	6815
$\gamma^{BS} \gamma^{BS} \rightarrow qqvv$	0.38%	32	0.37%	8
$\gamma^{BS} \gamma^{BS} \rightarrow qqqq$	<0.01%	0	<0.01%	0
$\gamma^{BS} e^- \rightarrow qqv$	4.04%	1711301	3.91%	46041
$\gamma^{BS} e^+ \rightarrow qqv$	4.02%	942574	4.01%	234665
$\gamma^{EPA} e^- \rightarrow qqv$	3.15%	416636	3.16%	11610
$\gamma^{EPA} e^+ \rightarrow qqv$	3.22%	236532	3.23%	59335
<b>Total:</b>	2.93%	3352635	2.24%	363070
signal				
$H_{inv} + qq$	42.16%	8023	42.04%	1388

Table 4: Efficiency and expected events number after preselection  $N_{pre}$  assuming integrated  $e^+e^-$  luminosity of  $2000 \text{ fb}^{-1}$  (negative polarisation) and  $500 \text{ fb}^{-1}$  (positive polarisation) collected at 1.5 GeV for each considered final state. Results for the signal were calculated assuming SM Higgs boson production cross section and  $\text{BR}(H \rightarrow inv) = 100\%$ .

### 3.2 Final selection

The second stage of the analysis was based on multivariate analysis and machine learning. The Boosted Decision Trees (BDT)[14] algorithm, as implemented in TMVA framework[15], was used, with 1000 trees and 5 input variables. The following parameters were selected as the BDT input variables:

1.  $E_{jj}$  – dijet energy,
2.  $m_{jj}$  – dijet invariant mass,
3.  $\alpha_{jj}$  – angle between the two reconstructed jets in the LAB frame,
4.  $m^{miss}$  – reconstructed missing mass,
5.  $p_t^{miss}$  – missing transverse momentum.

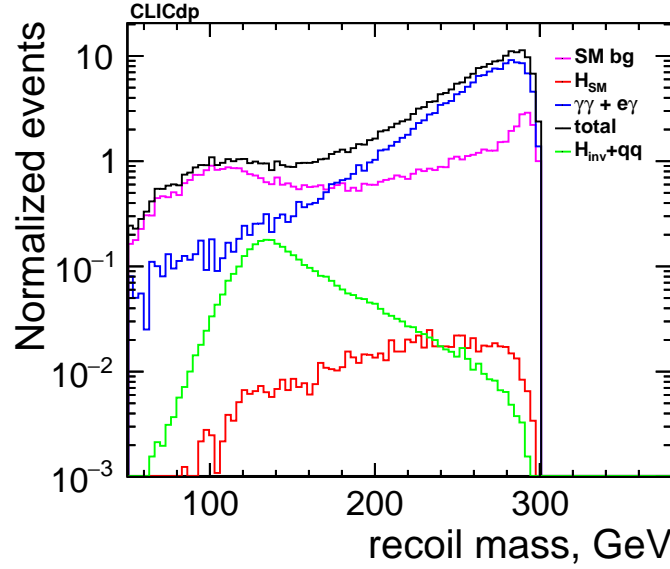


Figure 2: Distributions of the reconstructed invariant mass of the invisible Higgs boson decay products (recoil mass) expected for background (total background – black, SM background without Higgs particle production – pink, background of SM Higgs boson production and decays – red, photon interactions – blue) and signal (green) events after preselection cuts, assuming integrated  $e^+e^-$  luminosity of  $1000 \text{ fb}^{-1}$  collected at 380 GeV and  $\text{BR}(H \rightarrow \text{inv}) = 10\%$  for signal events.

The distributions of these variables for the signal and the background samples are shown in Figure 3. Various sets and numbers of parameters were tested; the above choice was selected as optimal, resulting in the most efficient event classification. Distributions of the BDT algorithm response for considered signal and background event samples (after preselection cuts) are shown in Figure 4. Consistent distributions obtained for training and test event samples confirm proper optimization of the BDT algorithm (no overtraining). Most of the background events can be easily distinguished from the signal, but there is also a significant contribution of background events for which BDT response values are positive, consistent with the response expected for signal events. This indicates that it is not possible to achieve full separation between the signal and the background processes. One should note that about 0.1% of SM Higgs boson decays result in fact in the invisible final state ( $H \rightarrow ZZ^* \rightarrow \nu\bar{\nu}\nu\bar{\nu}$ ), which is included in the background simulation.

In the final step of the analysis, we select the cut on the BDT response which gives the highest significance for the expected signal. The dependence of the signal significance at 380 GeV on the BDT algorithm response cut is shown in Figure 5, for the signal sample normalised to  $\text{BR}(H \rightarrow \text{inv}) = 1\%$ . The highest significance for invisible Higgs decays at 380 GeV CLIC is obtained for a BDT response cut of about 0.14, corresponding to a BDT selection efficiency for signal events of about 50% and background rejection efficiency of about 95%.

The same analysis procedure was applied for signal and background samples generated for CLIC running at 1.5 TeV, separately for two considered electron beam polarisation settings. Distributions of the BDT algorithm response for considered signal and background event samples (after preselection cuts) are shown in Figure 6. A similar level of signal-background separation is obtained for each polarisation.

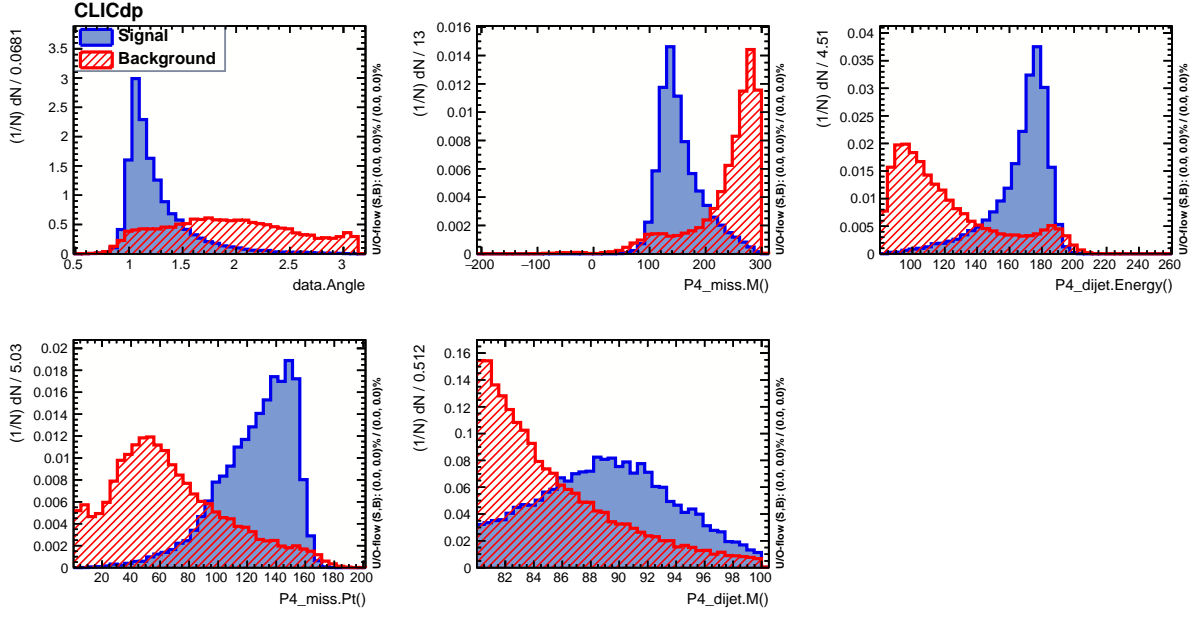


Figure 3: Distributions of the input variables for the BDT algorithm, for signal (blue) and background (red) event samples, for CLIC running at 380 GeV. Top row (from left): angle  $\alpha_{jj}$ ,  $m^{miss}$  [GeV],  $E_{jj}$  [GeV]; bottom row:  $p_t^{miss}$  [GeV],  $m_{jj}$  [GeV].

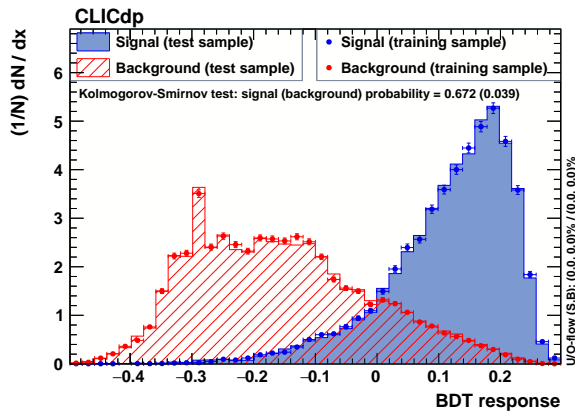


Figure 4: Distribution of BDT response for the signal (red) and the background (blue) for 380 GeV. Points stand for training samples and plain histograms for test samples.

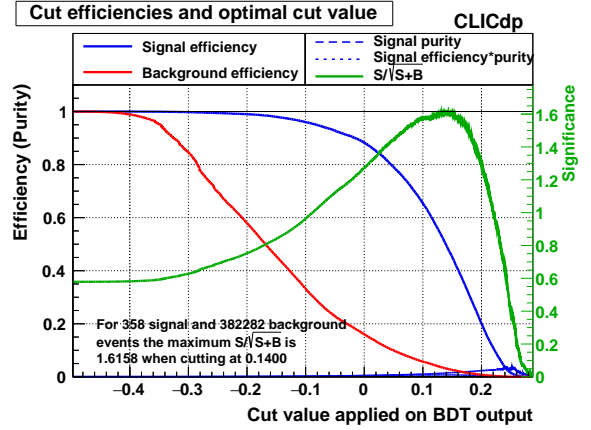


Figure 5: Significance for 380 GeV depending on BDT cut (green) assuming that only 1% of Higgs bosons decay invisibly.

## 4 Results

As a result of the preselection and selection procedures presented in the previous section, expected numbers of background events and efficiency of signal event selection are obtained. These can be translated into a constraint on the invisible branching ratio of the 125 GeV Higgs boson. For the first stage of the CLIC accelerator, assuming that the measured event distributions are consistent with the predictions of the Standard Model, the expected 95% CL limit<sup>6</sup> is:

<sup>6</sup> Assuming that one-side confidence limit of 95% corresponds to significance of 1.64.

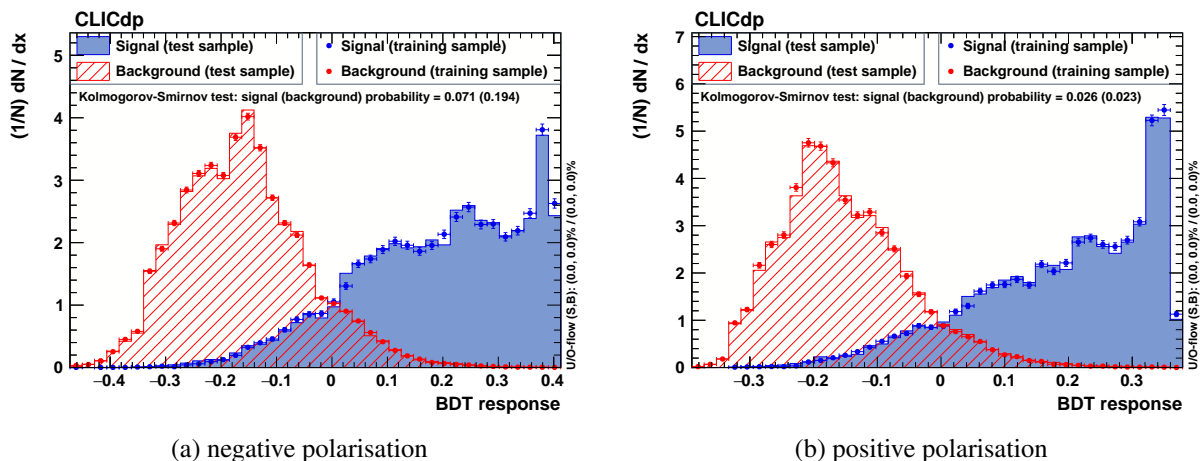


Figure 6: Distribution of BDT response for the signal (red) and the background (blue) for CLIC running at 1.5 TeV, with electron beam polarisation of  $-80\%$  (left) and  $+80\%$  (right). Points stand for training samples and plain histograms for test samples.

$$\text{BR}(H \rightarrow \text{inv}) < 1.0\%.$$

A significance above  $5\sigma$ , necessary to confirm the discovery of a new decay channel (and therefore also existence of new, invisible particles), is expected for an invisible Higgs boson branching ratio above  $3.1\%$ . Presented results, based on the fast simulation of the CLICdet detector model, are consistent with results of the previous study [16],  $\text{BR}(H \rightarrow \text{inv}) < 0.94\%$ , based on the full detector simulation, when the difference in the included background channels, collision energy and integrated luminosity is taken into account.<sup>7</sup>

The analysis procedure described above, developed to discriminate between the background of different SM processes and the signal of invisible Higgs boson decays was also used to estimate the expected sensitivity of CLIC experiment to production and invisible decays of a new scalar state. Signal simulation was based on the Standard Model implementation in WHIZARD (SM\_CKM model), with the modified Higgs boson mass and width (according to SM predictions for given mass). Samples of events with production of the new, hypothetical scalar particle  $H'$  with the emission of two quarks ( $e^+e^- \rightarrow H'Z \rightarrow \text{inv} + qq$ ) were generated for masses of the new scalar in the range 120-280 GeV (for the first stage of CLIC) and 150-1200 GeV (for the second stage). As for invisible SM Higgs boson decays, the produced particle  $H'$  was defined as stable in WHIZARD and PYTHIA, and non-interacting in DELPHES, to model its invisible decays. In this configuration,  $H'$  is always produced in WHIZARD with the assumed mass, corresponding to the narrow-width approximation.

After application of the same preselection cuts, we used the BDT algorithm, with the same set of input variables, for the final signal event selection. The algorithm was trained separately for each considered scalar mass (each generated signal sample). With the BDT response cut optimised for signal significance, we extract an expected limit on the cross-section for the production of the new scalar  $H'$  as a function of its mass, assuming its invisible decays,  $\text{BR}(H' \rightarrow \text{inv}) = 100\%$ . Obtained limits at 95% CL, relative to the expected cross section for the production of the SM-Higgs boson (for given mass), are presented as a function of the assumed scalar mass in Figures 7(a) and 7(b) for 380 GeV and 1.5 TeV, respectively.

The results indicate that the experiment at CLIC will be able to exclude new scalar production with rate of about 1% of the SM production cross-section for masses up to about 170 GeV (assuming only

<sup>7</sup>For collision energy of 350 GeV, assumed in [16], the expected cross section for  $e^+e^- \rightarrow q\bar{q}H$  is 93 fb, as compared to 82 fb at 380 GeV (see Table 1). In the previous analysis, beamstrahlung and EPA photon interactions were not included. The decrease of the cross section and the increase of the background events is compensated by factor 2 increase in the assumed integrated luminosity.

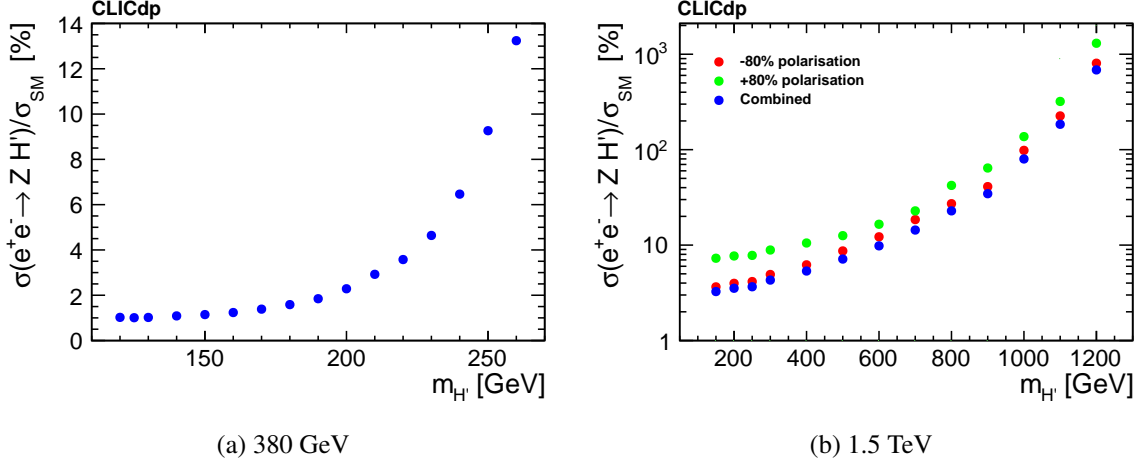


Figure 7: Expected limits on the production cross section of the new scalar  $H'$ , relative to the expected SM Higgs production cross section, as a function of its mass, for CLIC running at 380 GeV (left) and 1.5 TeV (right). New scalar is assumed to have only invisible decay channels,  $\text{BR}(H' \rightarrow \text{inv}) = 100\%$ .

invisible decay channels). For higher masses the experimental sensitivity decreases mainly due to the decreasing production cross section.

For the second CLIC stage sensitivity to production and invisible decays of the light Higgs-like scalars is smaller than at 380 GeV, mainly due to the decreasing signal cross section and higher background levels. The expected limit on the invisible decays of SM Higgs boson is about 3%. Assuming the production cross section given by the SM predictions, the second stage of CLIC will be sensitive to the new ‘invisible’ scalars up to about 1 TeV.

## 5 Interpretation

The expected limits on invisible decays of the 125 GeV Higgs boson and limits on the production of new “invisible” scalars, which were obtained in a model-independent approach, can also be used to constrain different BSM scenarios. As an example, we demonstrate the possibility of constraining parameters of the VFDM model [5, 6]. The Standard Model (SM) is extended by the spontaneously broken extra  $U(1)_X$  gauge symmetry and a Dirac fermion. To generate mass for the dark vector  $X_\mu$  the Higgs mechanism with a complex singlet  $S$  is employed in the dark sector. Dark matter candidates are the massive vector boson  $X_\mu$  and two Majorana fermions  $\psi_\pm$ . The spontaneous symmetry breaking in the dark sector results in an additional scalar state  $\phi$ . This state can mix with the SM Higgs field  $h$  implying existence of two mass eigenstates:

$$\begin{pmatrix} H \\ H' \end{pmatrix} = \begin{pmatrix} \cos \alpha & \sin \alpha \\ -\sin \alpha & \cos \alpha \end{pmatrix} \begin{pmatrix} h \\ \phi \end{pmatrix},$$

where we assume that  $H$  is the observed 125 GeV state. If  $\alpha \ll 1$ , it is SM-like, but it can also decay invisibly (to dark sector particles) via the  $\phi$  component ( $\text{BR}(H \rightarrow \text{inv}) \sim \sin^2 \alpha$ ). If  $H'$  is also light, it can be produced in  $e^+e^-$  collisions in the same way as the SM-like Higgs boson. We assume in the following that invisible decays to dark matter sector particles dominate for  $H'$  ( $\text{BR}(H' \rightarrow \text{inv}) \approx 100\%$ ). If this is the case,<sup>8</sup> the cross section for new scalar production corresponding to the limits presented in

<sup>8</sup>This assumption is a good approximation in a wide range of model parameters, although a small part of the new scalar decays must also be visible because otherwise the scalar would not be produced.

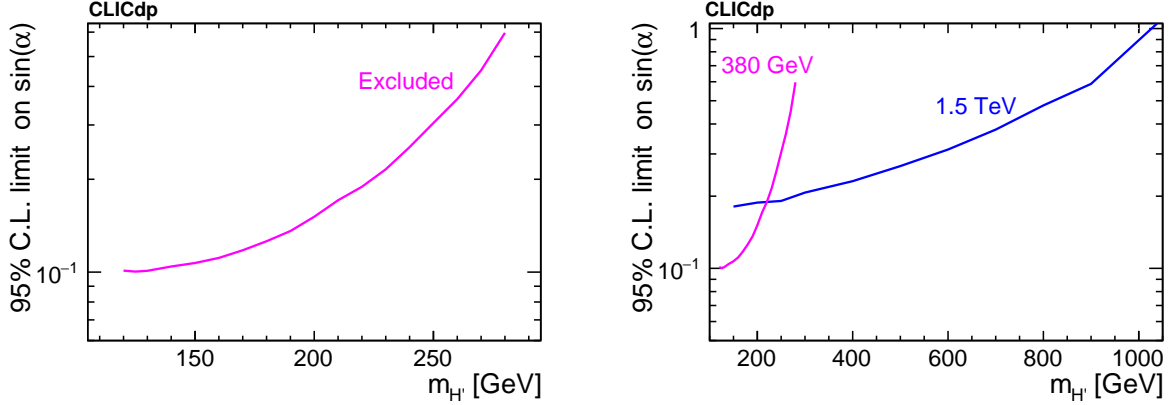


Figure 8: Expected limits on the sine of the scalar sector mixing angle,  $\sin \alpha$ , as a function of the  $H'$  mass, for CLIC running at 380 GeV (left and right plots) and 1.5 TeV (right plot).

the previous section can be written as:

$$\sigma_{H'} = \sigma_{SM}^{m_H=m_{H'}} \cdot \sin^2(\alpha),$$

where  $\sigma_{H'}$  is the cross-section for the production of a new scalar of mass  $m_{H'}$ , and  $\sigma_{SM}^{m_H=m_{H'}}$  is the cross-section for the production of the Higgs boson in the Standard Model with the same mass value. Limits on the sine of the mixing angle,  $\sin \alpha$ , resulting from the cross-section limits presented in Figure 7 are shown in Figure 8.

The mixing angle in the VFDM model can also be constrained by analysing the limit on the invisible branching ratio for the SM-like Higgs boson  $\text{BR}(H \rightarrow \text{inv})$ . When the contribution of the  $H'H'$  decay channel can be neglected, the invisible partial width of the Higgs boson,  $\Gamma_{\text{inv}}$ , is proportional to  $\sin^2(\alpha)$ , but depends also on other model parameters, in particular on the dark sector coupling constant,  $g_x$ , the mass of the vector dark matter,  $m_X$ , and the masses of the fermionic dark matter particles,  $m_{\Psi_-}$  and  $m_{\Psi_+}$ .<sup>9</sup> Constraints on the scalar sector mixing angle, resulting from the limits on the invisible decays of the SM-like Higgs boson expected at 380 GeV CLIC, are shown in Figure 9. Expected limits on  $\sin \alpha$ , plotted as a function of the  $\Psi_-$  particle mass, are based on the invisible decay widths<sup>10</sup> calculated with WHIZARD, for  $g_x = 1$  and  $m_X = m_{\Psi_+} = 200$  GeV. Also indicated in the Figure 9 are the indirect limits on the mixing angle, which can be set at CLIC from the analysis of the Higgs coupling measurements. Due to the mixing with the  $\phi$  state, all couplings of the SM-like Higgs boson to SM particles are scaled by  $\cos(\alpha)$ . In particular, the coupling of the Higgs boson to the Z bosons,  $g_{HZZ}$ , is given by:

$$g_{HZZ} = g_{HZZ}^{(SM)} \cdot \cos(\alpha).$$

It is expected that the experiment at 380 GeV CLIC will be able to measure  $g_{HZZ}$  in a model-independent approach with an accuracy of 0.6% [10]. If no deviations from SM are observed, the corresponding 95% C.L. limit on the mixing angle in the VFDM model is:

$$|\sin(\alpha)| < 0.14.$$

If the Higgs coupling fit is performed with the assumption that the Higgs boson couplings to all SM particles scale by the same factor,  $\kappa$ , much stronger constraints can be set [17]. After three CLIC running stages, the overall scaling of the Higgs boson couplings should be known to

$$\Delta \kappa = 0.06\%.$$

<sup>9</sup>The two fermionic states are defined in such a way that  $m_{\Psi_-} \leq m_{\Psi_+}$ .

<sup>10</sup>The scaling of SM (visible) decay width with factor  $\cos^2(\alpha)$  was neglected for the considered range of  $\sin \alpha$ .

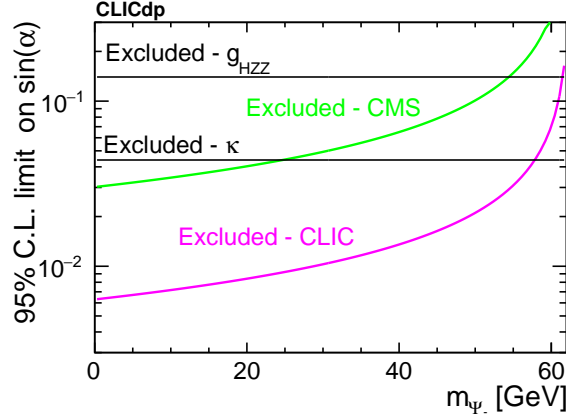


Figure 9: Expected limit on the sine of the scalar sector mixing angle,  $\sin\alpha$ , as a function of the  $\Psi_-$  particle mass of the VFDM model, for CLIC running at 380 GeV. Indicated by the green curve is the limit corresponding to the current constraint,  $\text{BR}(H \rightarrow \text{inv}) < 19\%$ , from the CMS experiment[4]. The horizontal line indicates the indirect limit expected from the measurement of the  $g_{HZZ}$  and  $\kappa$  couplings.

This corresponds to 95% C.L. limit on the mixing angle in the VFDM model of:

$$|\sin(\alpha)| < 0.044 .$$

Also indicated in Figure 9 is the limit on invisible Higgs boson decays from the CMS experiment,  $\text{BR}(H \rightarrow \text{inv}) < 19\%$  [4]. For masses of dark matter particles up to about 60 GeV, CLIC will allow to set much better constraints on the mixing angle in the scalar sector than it will be possible with indirect methods.

## 6 Summary

We studied the possibility of measuring invisible Higgs boson decays with CLIC running at 380 GeV and 1.5 TeV, taking background contributions from photon-photon and electron-photon interactions into account. The analysis is based on the WHIZARD event generation and fast simulation of the CLIC detector response with DELPHES. An approach consisting of a two step analysis was used to optimize separation between signal and background processes. The expected limit on the branching ratio for invisible Higgs boson decays is  $\text{BR}(H \rightarrow \text{inv}) < 1.01\%$ . This result is consistent with the previous analysis carried out with full simulation of the detector response. This shows that the fast simulation method used in the presented analysis should also be applicable to studies concerning new physics scenarios at CLIC. The branching-ratio and cross-section limits obtained in the model-independent approach can also be used to set limits on the different extensions of the Standard Model. In particular, constraints at the percent level can be set on the scalar sector mixing angle in “Higgs-portal” models.

## Acknowledgements

The work was carried out in the framework of the CLIC detector and physics (CLICdp) collaboration. We thank collaboration members for fruitful discussions, valuable comments and suggestions.

The work was partially supported by the National Science Centre (Poland) under OPUS research projects no 2017/25/B/ST2/00496 (2018-2021) and 2017/25/B/ST2/00191, and a HARMONIA project under contract UMO-2015/18/M/ST2/00518 (2016-2019).

## References

- [1] G. Aad et al., *Observation of a new particle in the search for the Standard Model Higgs boson with the ATLAS detector at the LHC*, Phys. Lett. **B716** (2012) 1, DOI: 10.1016/j.physletb.2012.08.020, arXiv: 1207.7214 [hep-ex].
- [2] S. Chatrchyan et al., *Observation of a new boson at a mass of 125 GeV with the CMS experiment at the LHC*, Phys. Lett. **B716** (2012) 30, DOI: 10.1016/j.physletb.2012.08.021, arXiv: 1207.7235 [hep-ex].
- [3] M. Tanabashi et al., *Review of Particle Physics*, Phys. Rev. D **98** (3 2018) 030001, DOI: 10.1103/PhysRevD.98.030001, URL: <https://link.aps.org/doi/10.1103/PhysRevD.98.030001>.
- [4] A. M. Sirunyan et al., *Search for invisible decays of a Higgs boson produced through vector boson fusion in proton-proton collisions at  $\sqrt{s} = 13$  TeV*, Phys. Lett. **B793** (2019) 520, DOI: 10.1016/j.physletb.2019.04.025, arXiv: 1809.05937 [hep-ex].
- [5] A. Ahmed et al., *Multi-Component Dark Matter: the vector and fermion case*, Eur. Phys. J. **C78** (2018) 905, DOI: 10.1140/epjc/s10052-018-6371-2, arXiv: 1710.01853 [hep-ph].
- [6] M. Iglicki, *Vector-fermion dark matter*, arXiv:1804.10289, 2018, arXiv: 1804.10289 [hep-ph].
- [7] D. Arominski et al., *A detector for CLIC: main parameters and performance*, CLICdp-Note-2018-005, arXiv:1812.07337, 2018, arXiv: 1812.07337 [physics.ins-det].
- [8] W. Kilian, T. Ohl, J. Reuter, *WHIZARD: Simulating Multi-Particle Processes at LHC and ILC*, Eur. Phys. J. **C71** (2011) 1742, DOI: 10.1140/epjc/s10052-011-1742-y, arXiv: 0708.4233 [hep-ph].
- [9] M. Moretti, T. Ohl, J. Reuter, *O'Mega: An optimizing matrix element generator*, AIP Conference Proceedings **583** (2001) 173, DOI: 10.1063/1.1405295.
- [10] A. Robson, P. Roloff, *Updated CLIC luminosity staging baseline and Higgs coupling prospects*, CLICdp-Note-2018-002, arXiv:1812.01644, 2018, arXiv: 1812.01644 [hep-ex].
- [11] J. de Favereau et al., *DELPHES 3, A modular framework for fast simulation of a generic collider experiment*, JHEP **02** (2014) 057, DOI: 10.1007/JHEP02(2014)057, arXiv: 1307.6346 [hep-ex].
- [12] E. Leogrande et al., *A DELPHES card for the CLIC detector* (2019), arXiv: 1909.12728 [hep-ex].
- [13] M. Boronat et al., *Jet reconstruction at high-energy lepton colliders*, Eur. Phys. J. **C78** (2016) 144, DOI: 10.1140/epjc/s10052-018-5594-6, arXiv: 1607.05039 [hep-ex].
- [14] B. Roe et al., *Boosted Decision Trees as an Alternative to Artificial Neural Networks for Particle Identification*, Nucl. Instrum. Meth. **A543** (2004) 577, DOI: 10.1016/j.nima.2004.12.018.
- [15] A. Hocker et al., *TMVA - Toolkit for Multivariate Data Analysis*, CERN-OPEN-2007-007, arXiv: physics/0703039, 2007, arXiv: physics/0703039 [physics.data-an].

- [16] M. A. Thomson, *Model-independent measurement of the  $e^+e^- \rightarrow HZ$  cross section at a future  $e^+e^-$ -linear collider using hadronic Z decays*, Eur. Phys. J. **76** (2016) 72,  
DOI: 10.1140/epjc/s10052-016-3911-5,  
URL: <https://doi.org/10.1140/epjc/s10052-016-3911-5>.
- [17] R. Franceschini et al., *The CLIC Potential for New Physics* (2018), ed. by J. de Blas,  
DOI: 10.23731/CYRM-2018-003, arXiv: 1812.02093 [hep-ph].